IMPROVED PERFORMANCES OF IPM MOTORS WITH TYPES OF DOUBLE V AND DELTA MAGNETS BY USING HIGH FLUX DENSITY MATERIALS

NÂNG CAO HIỆU SUẤT CỦA ĐỘNG CƠ IPM VỚI NAM CHÂM KIỂU VV VÀ TAM GIÁC BẰNG CÁCH SỬ DỤNG VẬT LIỆU CÓ MẬT ĐỘ TỪ THÔNG CAO

Bui Duc Hung[1,*], Bui Minh Dinh[1], Dang Quoc Vuong[1]

DOI: https://doi.org/10.57001/huih5804.59

ABSTRACT

The magnetic material has a big influence on the magnetic flux density in airgap of double V and delta magnets of IPM motors. Many papers used different materials to raise tthe performances of this machine such as materials of 35JN250, 35JNP5 and 50JNP7. In this paper, the material of Cobalt Steel-VaCoFlux with a high magnetic flux density is proposed for types of double V and delta magnets in the rotor to improve the efficiency of IPM motor. Two types of motor of 36 slots/6 poles with the slot fill winding and 72 slots/6 poles with the hairpin winding are presented to investigate the electromagnetic torque, efficiency, back electromotive force and magnetic flux density with different magnetic materials such as the silicon steel of M350-35A and VaCoFlux 50-0.35. The arrangement designs of the double V and delta magnets are also compared to evaluate and analyse the efficiency, torque and thermal. In addition, to improve the cogging torque due to the number of stators or slots, the step skew rotor slices are also arranged with different skewing angles to minimize the torque ripple. Finally, the cogging torque values and temperature distribution of two motors will be compared and discussed to see validation of a good agreement.

Keywords: *IPM Motor, Cobalt Steel-VaCoFlux, high flux density material, double V and delta (∇) magnets, Finite element method.*

TÓM TẮT

Vật liệu từ tính có ảnh hưởng lớn đến mật độ từ thông trong khe hở không khí của động cơ IPM với nam châm kiểu VV (double V) và tam giác (∇). Thép Cobalt - VaCoFlux với mật độ từ thông cao được đề xuất cho động cơ để cải thiện hiệu suất của động cơ. Hai động cơ với cấu trúc 36 rãnh/6 cực và 72 rãnh/6 cực với cách sắp xếp dây quấn kiểu chữ nhật (harpin) được giới thiệu để khảo sát mô-men điện từ, hiệu suất, sức phản điện động và mật độ từ thông ở tốc độ cơ bản với các vật liệu từ tính khác nhau như thép silicon M350-35A và VaCoFlux 50 - 0,35. Ngoài ra, rô to nam châm vĩnh cửu với thiết kế với kiểu VV và ∇ được so sánh để phân tích hiệu suất, mô-men và sự phân bố nhiệt độ. Để cải thiện mômen xoắn sinh ra do số lượng rãnh stato, rô to rãnh nghiêng được đề xuất để giảm thiểu độ nhấp nhô mômen với các góc nghiêng khác nhau. Cuối cùng, đặc tính mô-men xoắn và sự phân bố nhiệt độ của hai động cơ sẽ được so sánh và phân tích để đánh giá sự phù hợp của phương pháp đề xuất.

Từ khóa: *Động cơ nam châm vĩnh cửu gắn chìm, thép Cobalt-VaCoFlux, vật liệu mật độ từ cảm cao, nam châm kiểu VV và ∇, phương pháp phần tử hữu hạn.*

[1]School of Electrical and Electronic Engineering, Hanoi Unviversity of Science and Technology
[*]Email: hung.buiduc@hust.edu.vn
Received: 20/9/2022
Revised: 10/11/2022
Accepted: 22/11/2022

1. INTRODUCTION

The type of hairpin winding is used for the IPM motor to givie an increase of popularity [1, 2], especially for automotive traction motors. Due to their numerous advantages, it has obtained the reduction of manufacturing time, high fill factor, shorter end-winding overhang, and better high voltage protection. In addition, the hairpin windings consist of a plurality of accurately placed stator bars [3, 4]. However, these windings have also disadvantages of the complicated manufacturing and high cogging torque with a wider slot opening. Thus, in order to improve the torque ripple, an increase of number of stator slot is double for IPM of 200kW with 36 slots/6poles (36S6P)-slot fill winding and 72 slots/6 poles (72S6P)-hairpin winding. By using the material of VacoFlux for the stator, the magnetic flux density in air-gap needs to be increased. For a rectangle winding arrangement, the turn per slot will be limited in comparison with the type of a slot fill winding. For this way, the back electromotive force (EMF) can be improved significantly.

In the research, an IPM motor with the arrangements of double V (VV) and delta (∇) magnet rotor is developed to reduce the cogging

torque and improve the efficiency. In addtion, this way also allows to avoid the drawbacks of wide slot opening of stator slots. It should be noted that winding topologies will affect directly to the electromagnetic torque and efficiency of IPM machines. Hence, the electromagnetic performance of a multi-layered structrure is also investigated for this machine. Different step skewing models and topologies are then proposed to verify the validation of the torque and back EMF waveforms and torque harmonics. An IPM machine with a step-skewing magnet rotor is finally manufactured to validate obtained results via the finite element method (FEM).

2. DESIGN OF HAIRPIN AND SLOT FILL WINDINGS

The slot fill and hairpin windings of an IPM motor are designed as in Figure 1. The width of opening stator slots is 1.2mm for the slot fill winding (Fig.1a) and 5mm for the hairpin winding (Fig.1b). The permanent magnets with arrangements of V and ∇ shapes are pointed out in Figure 2. The main parameters of two different motors with 36S6P and 72S6P are also given in Table 1. Where the motor with 36 slots is made by silicon steel material and Cobalt steel is for the motor with 72 slots. The stack length is 51mm, the diameters of stator and rotor are respectively 250mm and 175mm, the air-gap length is 1mm, the thickness of the electrical steel sheet is 0.2mm, the amplitude of continuous phase current is 400A, the continuous rated power is 200kW and the maximum speed of the machines is 12000rpm.

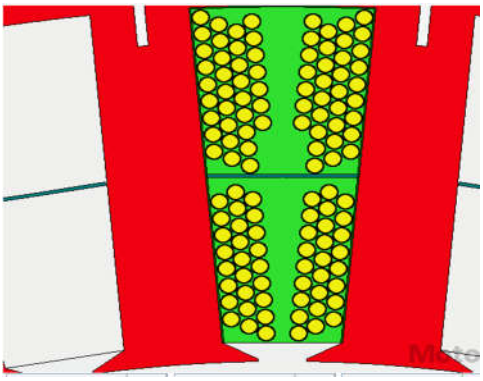

a) Slot fill winding (1.2mm opening)

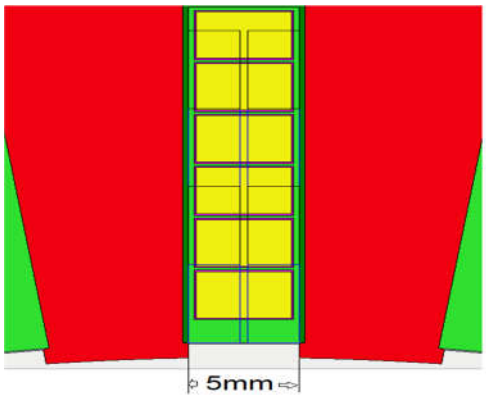

b) Hairpin winding (5mm opening)

Figure 1. Slot filled (a) and hairpin (b) windings

It should be noted that the main differences of these winding are the winding overhang, that is, slot openings and copper sizes of 15 (Φ0.85) and 4.3x3.3mm. For each applied voltage, the back EMF will be influenced by the type of different materials. This allows to estimate/define the peak magnetic field intensity (H), magnetic flux density (B) via the Ampere's and Faraday's laws.

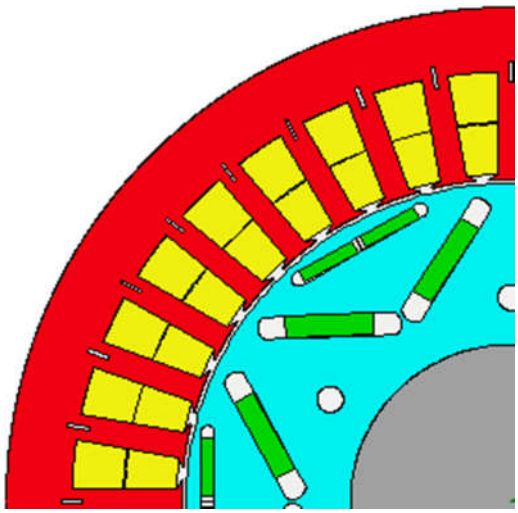

a) IPM 36 stator slots/6 poles-Delta

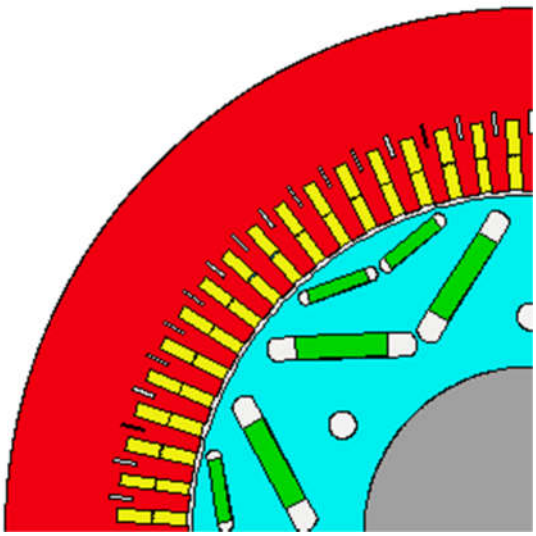

b) IPM 36 stator slots/6 poles-V

Figure 2. Slot fill and hairpin windings

The Curve of lamination materials of FeSi and VaCoFe from the manufacturer is presented in Figure 3 [11]. The iron core losses of lamination materials of M300-35A and VacoFlux with the different frequency values given from manufacturers is also pointed out in Figure 4 [11].

Table 1. Parameters of IPM motor with 36S6P-slot fill winding and 72S6P-hairpin winding

Parameter	Unit	36S6P (∇ shape)	72S6P (VV shape)
Stator Lam Dia	mm	230	230
Stator Bore Ds	mm	175	175

Airgap	mm	1	1
Stator slot opening width (t_s)	mm	1.2	5
Steel material		M350-35A	Vacoflux 50-0.35
Motor Length	mm	240	240
Stator Lam Length	mm	120	120
Magnet Length	mm	120	120
Magnet Segments		6	6
Rotor Lam Length	mm	100	100
Copper Winding	kg	10.8	9.5
Total Weight	kg	52	47
Copper size	mm	(Φ0.85)	4.3x3.3
Number Strands		15	1
Phases:		3	3
Turns:		6	6
Throw:		5	5
Parallel Paths:		2	2

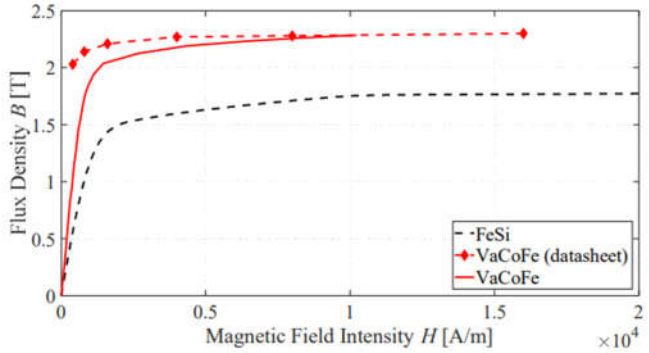

Figure 3. Curve of lamination materials of FeSi, VaCoFe from manufacturer [11]

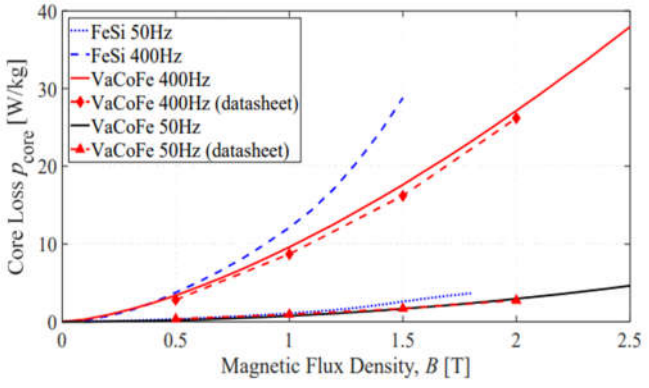

Figure 4. Iron losses of lamination materials of M300-35A and VacoFlux [11]

According to the data sheet from the manufacturer, the lamination material of VaCoFe is expected to reach around 2.0T at the B-H curve's knee-point. The curves obtained from experiments are considered in the optimization process to take the sensitivity of the material to the manufacturing processes into account.

3. FINITE ELEMENT APPROACH

An IPM motor with the rated power 200kW, rated torque 400Nm and the base speed of 5500rpm is applied to validate on the proposed method. In order to reduce the computation time, complexity and dimention of the studied model, only one pole pair of the machine is considered to mesh and simulate. A cut of the magnetic flux density distributions along the symmetry lines with the ∇ shape and VV shape is shown in Figure 5. The maximum value for the ∇ shape is 1.992T, whereas the VV shape is 2.407T. This can be confirmed that the structure of VV shape has a better magnetic flux density than the ∇ shape. The norm of the magnetic flux density in the stator teeth with the case of 36 slots/6 poles and 72 slots/ 6 poles is presented in Figure 6. It has shown that at the same rotor position, the norm value for the case of 72 slots/ 6 poles is bigger than the one of 36 slots/6 poles. In particular, the maximum value of magnetic flux density of 72S6P design is 1.8T higher than the one of 1.4T of the 36S6P design. However, the flux curve ripple of the 36S/6P design is double time than the one of 72S/6P designs. Parameter comparison of 36S6P-slot fill winding and 72S6P-hairpin winding is given in Table 2.

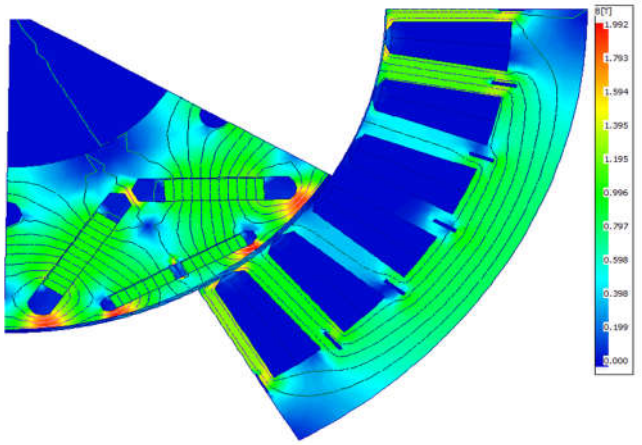

a) Stator with 36 slots/6 poles (∇ shape)

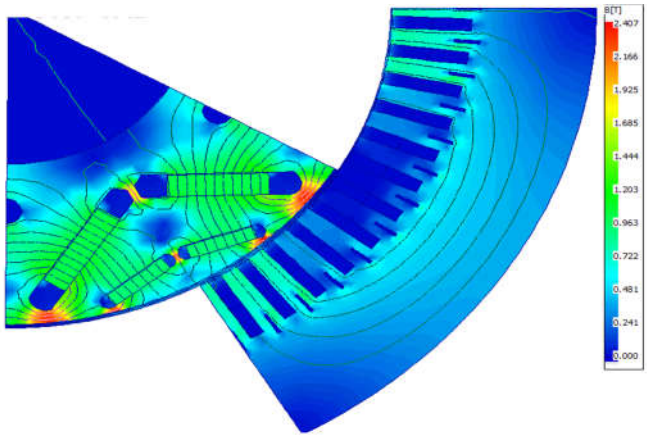

b) Stator with 36 slots/6 poles (VV shape).

Figure 5. Distributions of magnetic flux density with the ∇ shape (a) and VV shape (b)

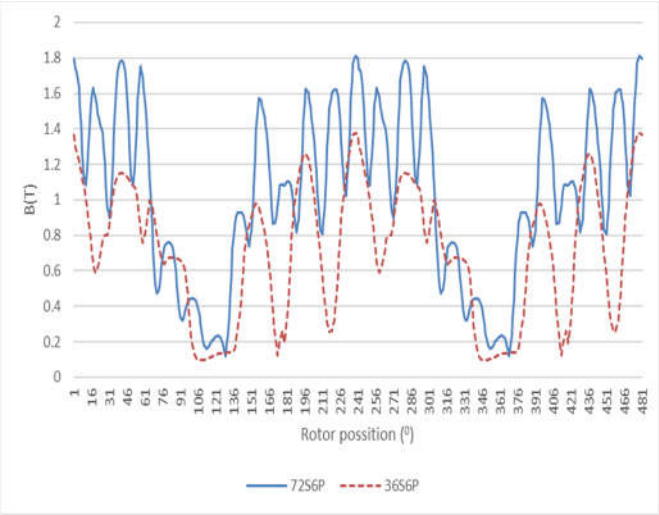

Figure 6. Norm of magnetic flux density

Table 2. Parameter comparison of 36S6P-slot fill winding and 72S6P-hairpin winding

Parameters	72S6P	36S6P	Unit
Maximum torque possible	435.71	407.22	Nm
Average torque	427.68	389.46	Nm
Average torque (loop torque)	424.79	388.62	Nm
Torque Ripple	16.544	79.045	Nm
Torque Ripple [%]	3.872	20.302	%
Cogging Torque Ripple	4.338	13.872	Nm
Cogging Torque Ripple (Vw)	4.6786	9.6663	Nm
Speed limit for constant torque	3364.9	2844.4	rpm
No load speed	12089	5739.5	rpm
Speed limit for zero q axis current	24024	6814.1	rpm
Electromagnetic Power	2.24E+05	2.04E+05	Watts
Input Power	2.32E+05	2.14E+05	Watts
Total Losses (on load)	9506.1	11069	Watts
Output Power	2.23E+05	2.03E+05	Watts
System Efficiency	95.906	94.827	%
Shaft Torque	425.36	387.51	Nm

4. ANALYSIS OF TORQUE PERFOMANCE

The instantaneous torque in time for the 36S6P with ∇ shape and 72S6P with VV shape is presented in Figure 7. The torque ripple of 72S6P design is relatively higher than the one of 36S6P design due to the flux concentration in the air gap.

In [11], for the material of VaCoFe, the higher saturation point allows higher flux concentration in the airgap. For the material of M350-35A, the torque ripple is higher than the one of the material of VacoFlux 50. In addition, the material of M350-35A has presented a peak-to-peak torque ripple of 79.04Nm (20.3%) and the material of VacoFlux 50 of 16.5Nm (3.8%). However, the torque ripple could be improved by using the skewing the rotor poles.

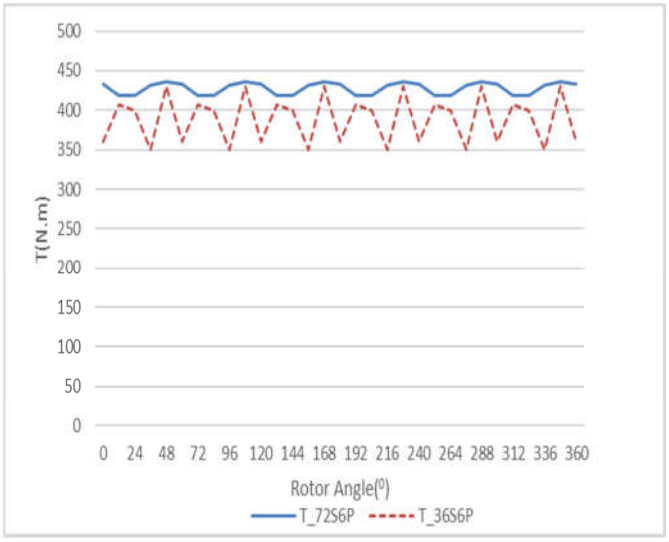

Figure 7. Torque ripple of 72S6P and 36S6P designs

As presented, the model of the slot opening is arranged along the motor axis, and the remain slots of the central position are the same. The cogging torque of IPM motor resulted from the interaction between the stator teeth and rotor magnetic poles can be expressed in the Fourier series [7], that is

$$T_{cog} = \sum_{i=0}^{n} T_{ci} \sin(iN\theta) \quad (1)$$

where i is the order of the harmonic component of cogging torque, T_{ci} is the amplitude of the i order of the cogging torque component, N is the least common multiple between the number of stator slots and rotor poles and θ is the mechanical angle of stator opening, which can be expressed as

$$\theta = 360 \frac{t_S}{\pi D_S} \quad (2)$$

where t_S is the slot opening width and D_S is the stator diameter.

In order to eliminate the cogging torque by using the stator slot-openings, a step skewing rotor with an angle shift of mechanical degree (β) is considered. For that, the cogging torque can be transformed to:

$$T_{cog} = \sum_{i=0}^{n} T_{ci} \sin(iN(\theta - \beta)) \quad (3)$$

If the rotor is divided into segments along the motor axial direction, and the relative shift angle between the adjacent and two rotor poles is the mechanical degree (δ_n), the resultant cogging torque can be expressed as:

$$T_{cog} = \sum_{i=1}^{n} T_{ci} \sum_{j=0}^{n-1} . \sin(iN(\theta - j\beta_n)) \quad (4)$$

The above equation can be simplified to

$$T_{cog} = \frac{1}{n} \sum_{i=1}^{n} T_{ci} \frac{\sin\frac{iN\beta_n n}{2}}{\sin\frac{iN\beta_n}{2}} \sin(iN(\theta - j\beta_n)) \quad (5)$$

Hence, by eliminating the i order of the cogging torque component, the theoretical shift angle β_n must fulfill the following requirements:

$$\sin\frac{iN\beta_n n}{2}=0 \quad (6)$$

By aplying the cogging torque for the straight skewing and V shape skewing magnet model, the conventional skewing model with straight skewing has a smaller shift angle than the V shape skewing model with the same total skewing angle.

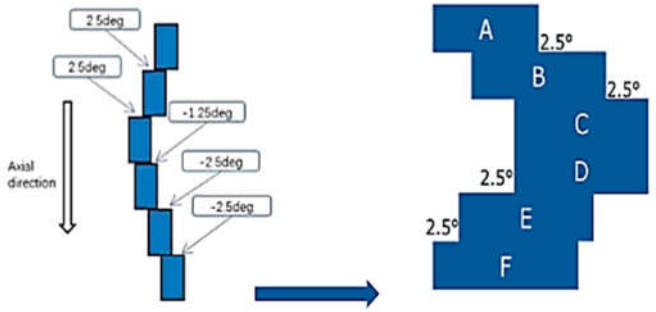

Figure 8. Cogging torque of slot fill and hairpin windings

The V shape model has more advantages than the straight skewing, because two harmonic orders can be eliminated together. For examples, the harmonic orders with mechanical degree of 1^0 or 3^0 is reduced to zero if they satisfy exactly the equation (6). The cogging torque of two different models are also shown in Figure 8 and Figure 9. The cogging torque of V shape skewing design is the lowest value because the double harmonic orders are eliminated in this model.

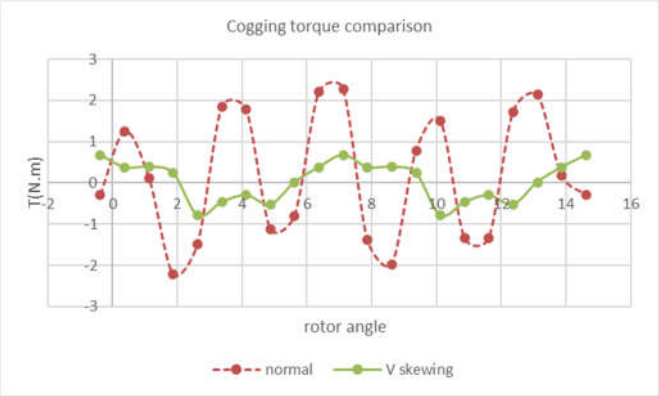

Figure 9. Cogging torque of two models

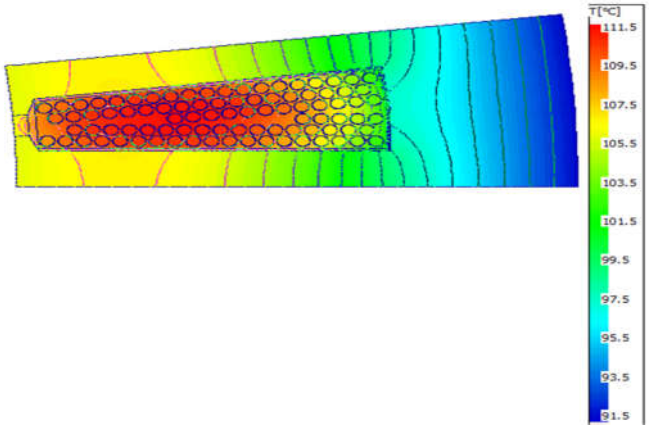

a) Slot fill winding design

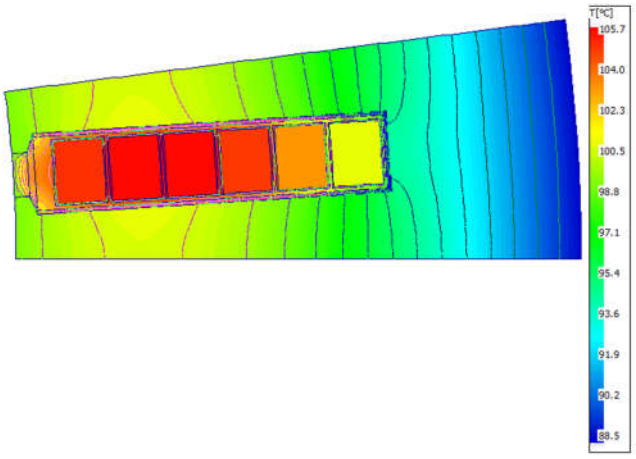

b) Hairpin winding design

Figure 10. Temperature distributions of slot fill and hairpin winding designs

Figure 10 shows temperature distributions of the type of different winding designs (slot fill winding and hairpin winding). It have shown that the hot spot of hairpin winding is 105.7^0C lower than the one of slot fill winding of 111.5^0C. Based on those results, the IPM with V skewing of hairpin winding design is selected for electric vehicle applications. The efficiency map of hairpin winding design has been pointed out with the speed range of 12000rpm and current density of 8.9A/m^2.

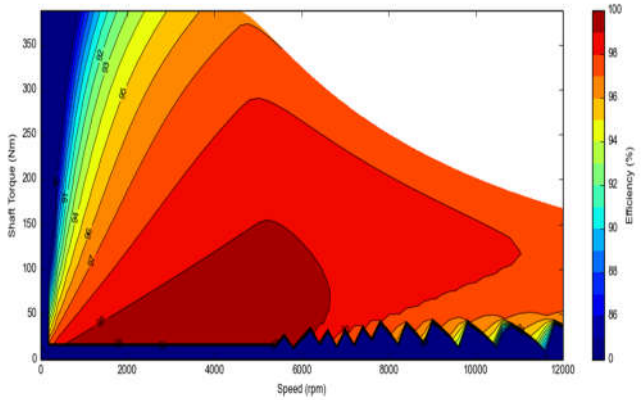

Figure 11. Efficiency map of hairpin winding design

5. SKEWING ROTOR TOPOLOGY FOR 72S6P-VV SHAPE

The six-segmented magnet prototype with VV shape is manufactured in Figure 12. Each segment with thickness of 20mm is skewed 1.5 mechanical degrees. To insert six segments simply, every segment block is designed one guide pin to fix a correct position when all segments assembly together. Parameters of stator lamination and stator slot are manufactured in Figure 13.

In order to verify the electromagnetic performances, the proposed IPM machine with the 72S6P design and distributed windings are built. The comparison of back EMFs with two different methods is illustrated in Figure 14, where the measured method with one circle of back EMF has been performed by the oscilloscope and recorded in

data files for plotting those curves. It can be seen that at based speed of 5500rpm, the back EMF waveform of simulated method is checked to be close the measured method.

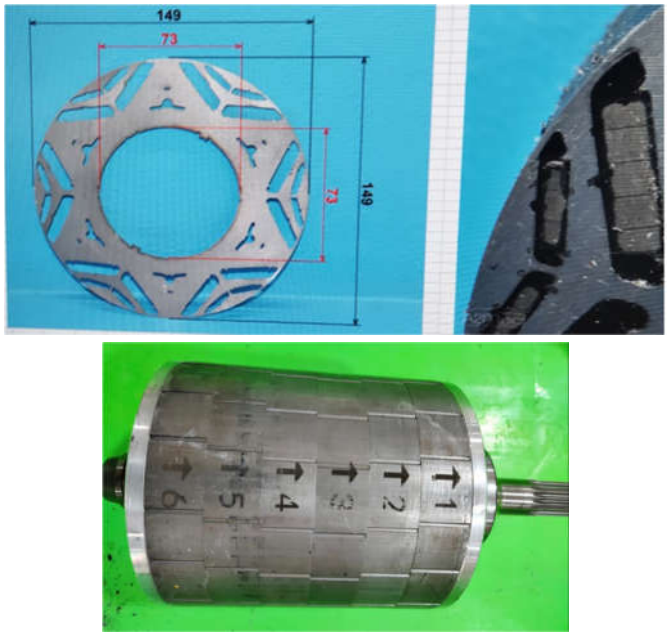

Figure 12. Rotor lamination, six-segmented magnet and VV skew magnet slices

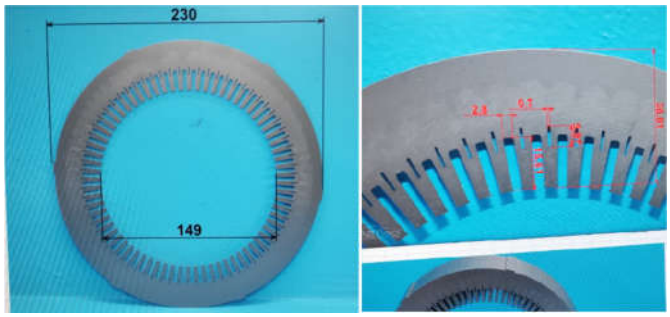

Figure 13. Parameters of stator lamination and stator slot

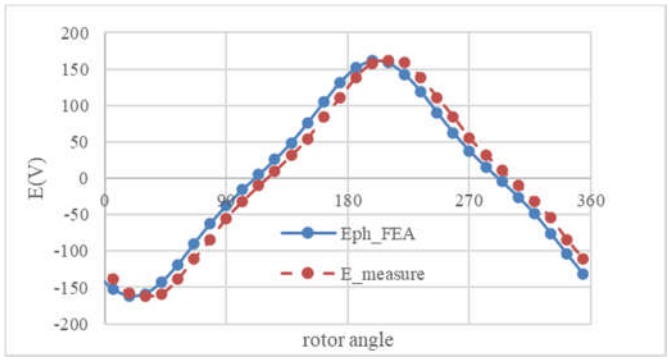

Figure 14. Comparison of back EMFs of IPM motor

6. CONCLUSIONS

The 72S6P and 36S6P designs of IPM motor of 200kW and 400Nm at the base speed 5500rpm with the slot fill and hairpin windings have been successfully implemented by the FEM. By using the material of high flux density with VacoFlux 50, the stator slots is increased from 36 slots to 72 slots, and the magnetic flux density of stator tooth is obtained from 1.1T to 1.8T as presented. The torque ripple is reduced significantly due to the stator slot opening being narrowed. The effect of material of VacoFlux 50 has been indicated via the distribution of magnetic flux density. In addtion, thermal simulation of two designs has been also investigated to find out the hot spot and maximum temperature of slot fill and hairpin windings, as well. The prototype of VV skewing magnet shape of IPM motor with the hairpin winding has been manufactured and assemblied. The comparison of back EMF waveforms obtained from two methods has been also pointed out to validate a good agreement.

REFERENCES

[1]. Liu C., Xu Z., Gerada D., Li J., Gerada C., Chong Y. C., Zhang H., 2019. *Experimental investigation on oil spray cooling with hairpin windings.* IEEE Trans. Ind. Electron., 67, 7343–7353.

[2]. Bhagubai P.P.C., Cardoso A.C., Fernandes J.F.P., 2020. *Cobalt Iron Core Impact on Optimal Design of an Interior Permanent Magnet Synchronous Motor for Competition Electric Vehicle*. In Proceedings of the 2020 2nd Global Power, Energy and Communication Conference (GPECOM), Izmir, Turkey.

[3]. Lee J., Yeo H., Jung H., Kim T.. Ro J., 2019. *Electromagnetic and thermal analysis and design of a novel-structured surface-mounted permanent magnet motor with high-power-density*. IET Electr. Power Appl., 13, 472–478

[4]. Junchen Zhao, Jin Wang, Libing Zhou, Weihua Huang, Yiming Ma, Zhiwei Zhang, 2019. *Cogging Torque Reduction by Stepped Slot-Opening Shift for Interior Permanent Magnet Motors*. 2019 22nd International Conference on Electrical Machines and Systems (ICEMS)

[5]. S. K. Lee, G. H. Kang, et al., 2012. *Stator and Rotor Shape Designs of Interior Permanent Magnet Type Brushless DC Motor for Reducing Torque Fluctuation*. IEEE Trans. Magn., vol. 48, no. 11, pp. 4662-4665, 2012.

[6]. Xiao Ge, Z. Q. Zhu, Graham Kemp, 2017. *Optimal Step-Skew Methodsfor Cogging Torque Reduction Accounting for Three-Dimensional Effect of Interior Permanent Magnet Machines*. IEEE Trans. Energy Convers., Vol.32, No.1, pp.222-232.

[7]. Volbers N., Gerster J., 2012. *High Saturation, High Strength Iron-Cobalt Alloy for Electrical Machines*. Proc. Inductica Cwieme Berl., 1–4.

[8]. Krings A., Boglietti A., Cavagnino A., Sprague S., 2017. *Soft Magnetic Material Status and Trends in Electric Machines*. IEEE Trans. Ind. Electron., 64, 2405–2414

[9]. Fernando N., Vakil G., Arumugam P., Amankwah E., Gerada C., Bozhko S., 2017. *Impact of Soft Magnetic Material on Design of High-Speed Permanent-Magnet Machines*. IEEE Trans. Ind. Electron., 64, 2415–2423.

[10]. Bucho L.F.D., Fernandes J.F.P., Costa Branco P.J., 2022. *Optimal Design of an Interior Permanent Magnet Synchronous Motor with Cobalt Iron Core.* Energies, 15, 2882.

THÔNG TIN TÁC GIẢ

Bùi Đức Hùng, Bùi Minh Định, Đặng Quốc Vương

Trường Điện - Điện tử, Trường Đại học Bách khoa Hà Nội